ISTITUTO NAZIONALE DI FISICA NUCLEARE
Laboratori Nazionali di Frascati

LNF-83/66(R)
18 Ottobre 1983

M. Sanzone: A REVIEW OF TWO BODY PHOTODISINTEGRATION OF DEUTERON AT INTERMEDIATE ENERGIES

Servizio Documentazione
dei Laboratori Nazionali di Frascati
Cas. Postale 13 - Frascati (Roma)

INFN - Laboratori Nazionali di Frascati
Servizio Documentazione

LNF-83/66(R)
18 Ottobre 1983

A REVIEW OF THE TWO BODY PHOTODISINTEGRATION OF DEUTERON AT INTERMEDIATE ENERGIES

M. Sanzone
INFN - Sezione di Genova, and Istituto di Scienze Fisiche dell'Università di Genova

CONTENTS:

1. - INTRODUCTION

The deuteron, the simplest of all nuclear system, has the same importance for nuclear theory as the hydrogen atom has for atomic theory.

The fundamental rule of this nucleus is due to several reasons, some of them are obvious, all of them are in any case immediately evident. As the deuteron consists of a proton and a neutron, in dealing with such a two-body problem, the wave functions can be rigorously calculated, if the forces are known.

This means, on the other side, that, when the interaction is well known, as is the case of the electromagnetic interaction, the comparison between theory and experiment is itself a test of the forces between nucleons. Moreover only one-or two-body interactions are involved in the process, no many-body problems complicate the calculations, so the theory does not need too many approximations and the results are more direct and clean.

From the experimental point of view, as the process gives a break-up of the nucleus in two particles only and no other reaction channels are possible, at least until the excitation energy is lower than the pion production threshold, the measurement of the yield of protons emitted is a direct measurement of the deuteron disintegration cross section. Moreover, since the deuteron has no bound excited states, the measurement of the proton energy and direction is also a measurement of the incoming probe energy. This is very important when a continuous spectrum is used, as in the case of bremsstrahlung photon beam.

The last remark concerns the binding energy: apart from ^{9}Be for the break-up in $2\alpha + n$, ^{2}H is the only stable nucleus with a small binding energy. This makes possible to study the transition properties to high level continuum states of the nucleus, by using, for instance, available gamma sources from nuclear reactions.

It appears now evident why a large part of the literature on photonuclear physics consists of papers involving electromagnetic interactions on deuteron and in particular involving the photodisintegration of deuteron, the simplest process to be experimentally investigated. Even if a deuteron target is not a simple target, many experiments have been performed using almost all kind of accelerators and techniques. It is not without significance that everytime a new generation of accelerators appears in the history of nuclear physics and everytime new conceptions of the nucleon-nucleon force (isospin or momentum dependent, pion exchange and so on) or of the nuclear system (isobar configurations, quarks and so on) are proposed, the deuteron is taken as a test case. We find in the more recent literature even a tentative to introduce quark-gluon degrees of freedom to describe the deuteron nuclear system at interaction energy below 100 MeV[1].

"Disintegration of the diplon by γ-rays" is the first experimental historically in order to study the nuclear photoeffect. It was carried out by J. Chadwick and M. Goldhaber in 1934[2], using γ-rays of 2.62 MeV of Thorium C" and an ionization chamber to detect protons. Only two years earlier the discovery of the neutron by Chadwick[3] has made possible a more detailed picture of the constitution of the nucleus and only one year earlier Heisenberg[4], Majorana[5] and Wigner[6] tried to describe the behaviour of protons and neutrons and their interaction in the nucleus by the methods of quantum mechanics. In the same year of photodisintegration experiment appeared also the first theoretical work on this process, the "Quantum theory of the diplon" by H. Bethe and R. Peierls[7]. So both the first experiment and the first theory on photodisintegration of Deuteron belong to the dawn of the nuclear physics history and this shows again the importance of the investigation on this nucleus.

2. - PRESENT STATUS OF THE THEORY

It would be too long and without usefulness to discuss here about all the theoretical approaches and calculations on deuteron photodisintegration, that have appeared in the literature. Therefore, I will report only on those that are, in my opinion, more significant or useful to understand the complex problem of the structure of this nucleus and its photoeffect. Moreover I will dedicate the main part of this section to the photoeffect at intermediate energies, it means between 10 MeV and the threshold of pion production, leaving the discussion of the high energy photodisintegration to the end of this section.

In the already mentioned work of Bethe and Peierls[7] the total cross section for the photoemission of proton from the deuteron is derived from the analogy between this process and the photoelectric effect of an atom and it is written

$$\sigma_{BP}(h\nu) = \frac{\pi^3 e^2 \nu}{c} \left| Z_{OE} \right|^2 \qquad (1)$$

where $h\nu$ is the photon energy and Z_{OE} is the overlap integral between the ground state proton wave function u_o and the wave function Φ_k of the proton in the final state with k wave number for E1 transition

$$Z_{OE} = \int u_o(r) \frac{1}{2} z \; \Phi_k(r) \, . \qquad (2)$$

To evaluate this overlap integral the authors make two approximations:

- For the ground state the asymptotic expression of the wave function at large distance is taken, assuming that for low $h\nu$ values the cross section is not sensitive to the inner part wave function

$$u_o(r) = \sqrt{\frac{\alpha}{2\pi}} \; \frac{e^{-\alpha r}}{r} \qquad (3)$$

where α is related to the binding energy ε of deuteron

$$\alpha = \left(\frac{M\varepsilon}{\hbar}\right)^{1/2} . \qquad (4)$$

Obviously this assumption is not valid for $r < a$ (where a is the range of the assumed potential, $a \simeq 10^{-13}$ m) and this expression does not give a finite value for $r = 0$. Therefore the approximation cannot be valid for photon energies far from the threshold.

- The final state of the proton is the wave function of a free particle with wave number k

$$\Phi_k = (2\pi)^{-3/2} \, e^{i(\vec{k}\cdot\vec{r})} \qquad (5)$$

(the overlap integral for E1 transition has a value $\neq 0$ only for a final p-state). Again, at radii smaller than a, this is not true because the proton is subject to a strong force, but for small energies the approximation does not differ much from the exact result.

Fifteen years later Bethe and Longmire[8] have improved the above calculations by taking the effective range (ER) into consideration. Let $u_i(r)$ be the radial wave function (multiplied by r) that satisfies the radial Schrodinger equation for a state with k wave number

$$\frac{d^2u_i}{dr^2} + k^2u_i - V(r)u_i = 0 \tag{6}$$

V is the potential energy multiplied by $M/\hbar^2$, and $\psi_i(r)$ the asymptotic behaviour of $u_i(r)$ for large distances. Some assumptions have to be made concerning these functions :

- u and ψ differ only inside the intrinsic range of the nuclear forces;
- in this region u and ψ depend only very slightly on the energy because kr is small and the potential energy is much larger than k^2/M.

As a consequence it is possible to write

$$\int_0^\infty (\psi_i\psi_j - u_iu_j)\,dr = \int_0^\infty (\psi_o^2 - u_o^2)\,dr = \text{cost} = \frac{1}{2}r_o \tag{7}$$

where u_o and ψ_o are the wave function refering to zero energy. The quantity r_o is independent of the energy, and has the dimension of a distance. It represents the difference between u and ψ inside the intrinsic range of the nuclear forces and should be zero for zero-range nuclear forces. For this it is called the "effective range" (ER)[8-10].

Taking into account the "effective range", Bethe and Longmire wrote the ground state wave function

$$u_o(r) = \sqrt{\frac{\alpha}{2\pi}}\,\frac{e^{-\alpha r}}{r}\,(1 - \alpha r_o)^{-1/2}\,. \tag{8}$$

The wave function of the final state is again the P wave function for a free particle as only E1 transition is taken into account. As a consequence the cross section becomes

$$\sigma_{ER} = \sigma_{BP}/(1 - \alpha r_o) \tag{9}$$

where σ_{BP} is the Bethe-Peierls cross section (1), it means for zero-effective range. The value of the effective range was found to be independent of the shape of the assumed nuclear potential (square well, exponential, Yukawa) and it was evaluated to be

$r_o = 1.59 \times 10^{-13}$ cm, so that the cross section for the photoelectric effect becomes

$$\sigma_{ER}(h\nu) = 1.586\, \sigma_{BP}(h\nu) . \tag{10}$$

At about the same time Levinger[11], Schiff[12] and Marshall and Guth[13] derived the photoelectric effect cross section, using Hulthén wave function for the ground state of the deuteron

$$u_o(r) = \sqrt{\frac{\alpha}{2\pi}}\,\frac{1}{r}\,(e^{-\alpha r} - e^{-\beta r})(1 - \alpha r_o)^{-1/2} \tag{11}$$

where β is determined from the effective range as $5.8\,\alpha$.

The cross section for the dipole term of the photoelectric effect is given by

$$\sigma_H(h\nu) = \sigma_{ER}(h\nu)\left\{1 - \left[\frac{\eta}{\alpha^2/\beta^2 - 1 + \eta}\right]^2\right\}^2 . \tag{12}$$

The Hulthén potential is a good approximation of the Yukawa potential and seems to give a result similar to that of an exponential potential, at least up to about 100 MeV[13] as shown in Fig. 1a. On the contrary the square-well potential gives appreciable difference[13] (Fig. 1b).

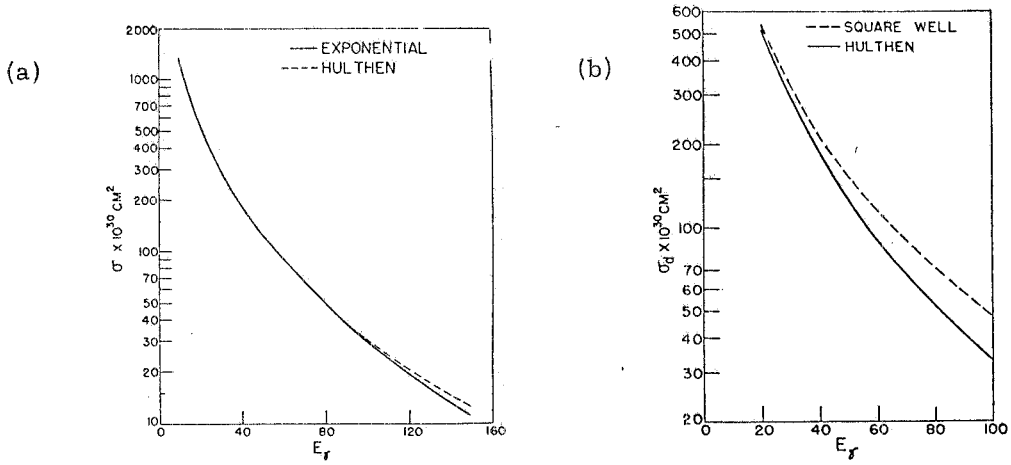

FIG. 1 - Total cross section for $r_o = 1.74 \times 10^{-13}$ cm. Comparison of Hulthén potential with Exponential (a) and Square-well (b) potentials.

Levinger used an effective range $r_o = 2.5 \times 10^{-13}$ cm and evaluated only the electric dipole contribution. Schiff and Marshall et al. used two values for the effective range $r_o = 1.56 \times 10^{-13}$ cm and $r_o = 1.74 \times 10^{-13}$ cm and evaluated electric dipole and quadrupole contributions, no magnetic dipole. The two values of r_o do not give appreciable differences at least up to 80 MeV[13] as shown in Fig. 2a and 2b.

(a)

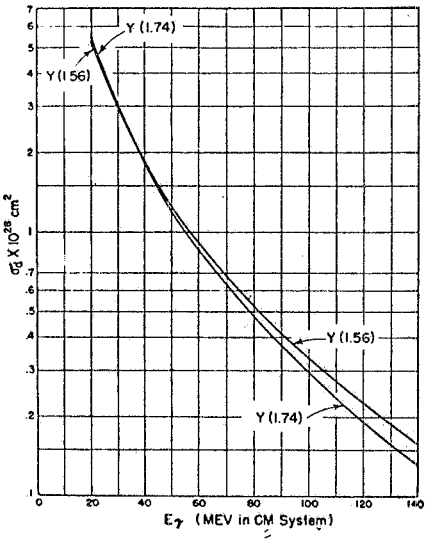

(b)

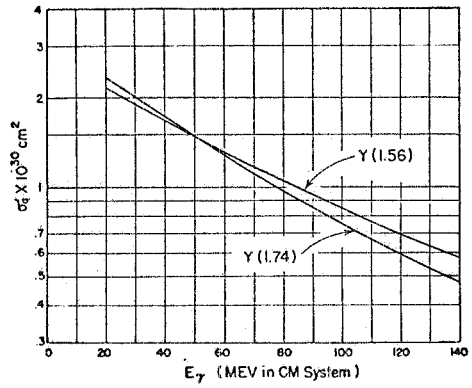

FIG. 2 - Total photoelectric dipole (a) and quadrupole (b) cross sections for effective ranges 1.56×10^{-13} cm and 1.74×10^{-13} cm.

At this point it is useful to make remarks concerning the calculations previously reported. The introduction of the effective range increases in any case the cross section, independently from the assumed potential, at least for energies lower than 100 MeV.

The approach of Bethe and Longmire gives a constant factor, the calculation using the Hulthén potential gives on the contrary a factor that depends on the photon energy especially at high energy.

This result should be expected because Bethe and Longmire take into account the difference between the actual wave function and the asymptotic wave function just renormalizing the latter one without changing the shape. In the calculations of Levinger, Schiff, and Marshall and Guth the finite range not only changes the normalization constant, but also the shape of the assumed wave function. Moreover a photon with higher energy (it means with lower wave length) becomes more and more sensitive to the inner part of the ground state wave function of the nucleus, it means more and more sensitive to the difference between the actual and asymptotic wave function and as a consequence the cross section deviates more from that one evaluated with zero-range assumptions.

In Fig. 3 is presented the ratio between the cross sections evaluated by taking in to account the effective range and the zero-range cross section. Also the behaviour of the average values of the experimental data (that will be discussed in the next session) is reported. It is evident that the introduction of the effective range enables the theory to reproduce the experimental data at least up to about 40 MeV. The strong discrepancy at the threshold is due to a magnetic dipole transition that dominates over the electric dipole transition, since the S-wave for the final state in M1 transitions is more easily emitted at very low energies than a P-wave for E1 transitions[14]. For photon energy much larger than the binding energy the ratio between M1 and E1 cross sections is

about 1 percent.

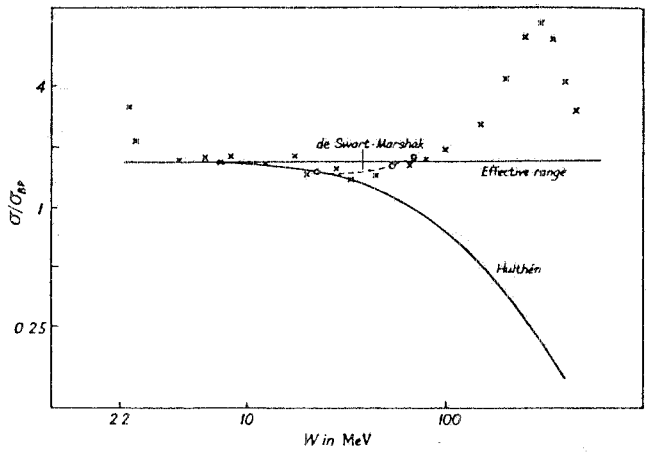

FIG. 3 - Ratio between σ and σ_{BP} total cross sections. The crosses show experimental data; the horizontal line and the curve represent respectively σ_{ER} (10) and σ_{H}(11).

The first very detailed and accurate theoretical analysis of deuteron photodisintegration was performed by Partovi[15]. The wave functions of the deuteron and the continuum state[16] are calculated using Hamada-Johnston potential that provided a good fit for the n-p scattering below 315 MeV

$$V_{HJ} = V_c + V_T S_{12} + V_{LS}(\vec{L}\cdot\vec{S}) + V_{LL} L_{12} \tag{13}$$

where

$$S_{12} = \sqrt{24\pi}\left[\vec{\sigma}_1 \times \vec{\sigma}_2 \times Y(\vec{r})\right], \tag{14}$$

$$L_{12} = (\vec{\sigma}_1\cdot\vec{\sigma}_2)L^2 - \frac{1}{2}\left[(\vec{\sigma}_1\cdot\vec{L})(\vec{\sigma}_2\cdot\vec{L}) + (\vec{\sigma}_2\cdot\vec{L})(\vec{\sigma}_1\cdot\vec{L})\right]. \tag{15}$$

The various terms represent in successive order the central, tensor, linear spin-orbit and quadratic spin-orbit potential. The interaction Hamiltonian is written

$$H^{int} = -\int \vec{j}(\vec{x})\cdot\vec{A}(\vec{x})\, d\vec{x}\,. \tag{16}$$

The vector potential operator of the radiation field $\vec{A}(\vec{x})$ is given in plane waves of circular polarization

$$A(x) = \frac{1}{\sqrt{\Omega_N}} \sum_{\omega} \sum_{=\pm 1} \left(\frac{2\pi}{\omega}\right)^{1/2} \vec{\varepsilon}_\mu e^{i\vec{\omega}\cdot\vec{x}} \tag{17}$$

where Ω_N is the normalization volume, ε_μ are spherical unit vectors. $\vec{\varepsilon}_\mu e^{i\vec{\omega}\cdot\vec{x}}$ is expanded in electric and magnetic multipoles but in the calculations only multipole terms up to the dipole-octupole interference are taken into account. $\vec{j}(\vec{x})$ is the current density operator associated with the n-p system and it has to fulfil the well known conservation requirement of the electric charge or continuity equation

$$\vec{\nabla}_x \cdot \vec{j}(\vec{x}) = -i\left[H_{n-p},\ \varrho(\vec{x})\right] \tag{18}$$

where H_{n-p} and $\varrho(\vec{x})$ are the Hamiltonian and the charge density operator for the neutron-proton system without taking into account any nucleon electromagnetic structure. Moreover as the current density and charge operators are sum of single particle terms, no meson exchange contribution is "explicitely" taken into account, as we will see later.

The photodisintegration cross section is calculated at several laboratory photon energies between 10 and 140 MeV and calculations are done in several approximation to exhibit the effect of various terms.

Dipole transitions account for the main part of the total cross section at all energies. At 20 MeV electric dipole plays the dominant role, at higher energies other multipole effects become increasingly important. The differential cross section is written (in the centre of mass system for upolarized photons)

$$\frac{d\sigma(\theta)}{d\Omega} = a + b\sin^2\theta + c\cos\theta + d\sin^2\theta\cos\theta + e\sin^4\theta\,. \tag{19}$$

The total and the differential cross sections are compared with the existing experimental data in Figs. 4 and 5. As will be discussed in the next section there is a vast discrepancy among different experimental data, never

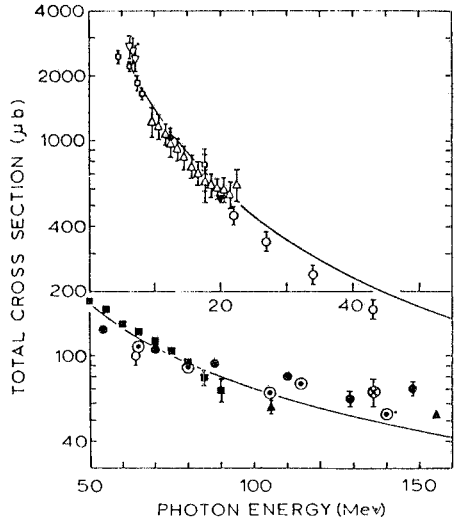

FIG. 4 - Total cross section. Comparison between Partovi's calculations and experimental data, from ref. (15).

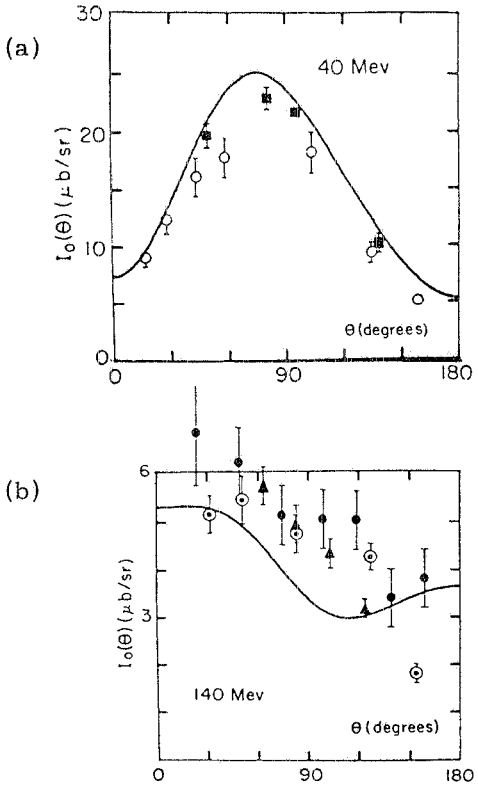

FIG. 5 - Differential cross section for E_γ = 40 MeV (a) and E_γ = 140 MeV (b). Notation as Fig. 4.

theless good agreement seem to be at low energy, but at high energy (mainly above 100 MeV) at least the theoretical differential cross section appears clearly in disagreement with the average behaviour of the experimental data.

After Partovi's calculations we had to wait at least ten years to find in the literature a substantial and effective improvement in the calculations of deuteron photodisintegration at intermediate energies. I refer myself to the work of Arenhövel and collaborators that started around 1973[17] and continued until today[18, 19] when for the first time in this energy range(x) both isobar configurations of the nucleus (IC) and meson exchange current (MEC) were explicitely included in the electromagnetic transition amplitude and the implication of these ingredients was extensively studied using a variety of realistic NN potentials. Moreover Arenhövel, discussing the effective role and the implication of Siegert's theorem[21] in the electric transition expressions, puts very clearly in evidence the implicit and explicit contributions of exchange currents to the deuteron photodisintegration process[22].

The notion that nuclear forces are caused by the exchange of mesons between nucleons suggests that together with the currents associated with the motion of the nucleons, an additional meson current (so called meson exchange current) must be taken into account in the electromagnetic transition amplitude.

The assumption is made that the operator describing exchange effects involve only the coordinates and spins of the nucleons and that exchange effects are two-body effects.

As the exchange effect is expected to depend in some way on the interaction between nucleons, the exchange current has not the simple one-body additivity property which is usually associated with electric currents occurring in system described by the Schrödinger equation.

As a consequence of these assumptions and deductions the interaction Hamiltonian H^{int} is now written as the sum of two parts

$$H^{int} = H^{int}_{[1]} + H^{int}_{[2]} \tag{20}$$

where H^{int}_{1} is the already mentioned interaction Hamiltonian of Partovi that contains the normal one-body current

$$H^{int}_{[1]} = - \int \vec{J}_{[1]}(\vec{r}) \cdot \vec{A}(\vec{r}) \, d\vec{r} \tag{21}$$

(x) For thermal n-p capture MEC effects have been considered before by Riska and Brown[20].

and $H^{int}_{[2]}$ takes into account the additional two-body current density operator and describes the influence on the electromagnetic interaction when the relative distance $\vec{r}_{ij}$ between the two nucleons changes

$$H^{int}_{[2]} = - \int \vec{J}_{[2]}(\vec{r}, \vec{r}_{ij}) \cdot \vec{A}(\vec{r}) \, d\vec{r} . \tag{22}$$

Following Partovi's notation the vector potential operator is expanded in electric and magnetic multipoles and again it is taken into account that the current density operator has to fulfil the continuity equation (18). At this point it is useful to do some remarks concerning the meaning of the current density operators.

In the long wave-length limit the electric multipoles can be expressed in terms of charge multipoles using the continutiy eq. (18). This is the content of Siegert's theorem[21]. Moreover I will recall the Siegert's hypothesis[21] that in the non-relativistic limit, the electric charge density remains unchanged by MEC effects, i. e. is well described by the classical one-body point particle densities. This means that exchange meson currents are taken into account already by a part of the "normal" interaction Hamiltonian (21) when one uses the substitution

$$\vec{\nabla}_r \cdot \vec{J}_{[1]}(\vec{r}) = -i \left[H, \varrho(\vec{r}) \right] \tag{23}$$

and that this expression must in effect be written

$$\vec{\nabla}_r \cdot \left[\vec{J}_{[1]}(\vec{r}) + \vec{J}_{[2]}(\vec{r}) \right] = -i \left[H, \varrho(\vec{r}) \right] . \tag{24}$$

This must be taken into account if MEC effects are evaluated in addition with $H^{int}_{[2]}$ to avoid double counting of the mesonic effect. This is called the Siegert's correction[22].

As it was very clearly deduced by Arenhövel[22] this continuity equation corresponds to the two equations

$$\vec{\nabla}_r \cdot \vec{J}_{[1]}(\vec{r}) = -i \left[T_{[1]}, \varrho(\vec{r}) \right], \tag{25}$$

$$\vec{\nabla}_r \cdot \vec{J}_{[2]}(\vec{r}) = -i \left[V_{[2]}, \varrho(\vec{r}) \right] \tag{26}$$

where $T_{[1]}$ is the one-body kinetic energy operator and $V_{[2]}$ is the two-body interaction potential. Thus, if the two-body potential $V_{[2]}$ is isospin and/or momentum dependent, the first term of eq. (26) cannot vanish identically.

To see how much mesonic effect is already included by the Siegert's theorem in the normal $H^{int}_{[1]}$, in Figs. 6 and 7 are presented the results of Arenhövel[19, 22] calculations respectively of the total cross section and the angular distributions for d(γ, p)n,

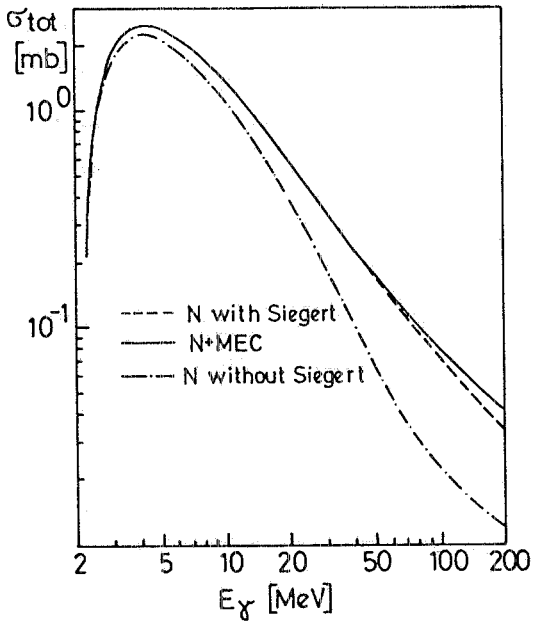

FIG. 6 - Total cross section for normal theory without and with Siegert operator and with additional MEC from ref. (19).

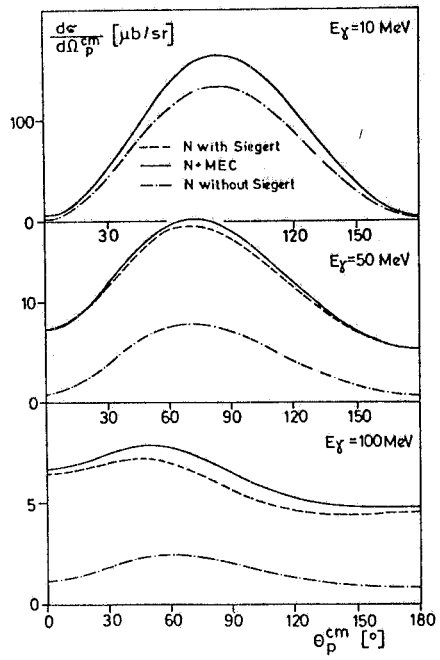

FIG. 7 - Angular distributions for E_γ = 10, 50 and 100 MeV. Notation as Fig. 6.

in several conditions, i. e. using only $H^{int}_{[1]}$ with and without Siegert's theorem and with the additional exchange contributions due to $H^{int}_{[2]}$. One readily sees that large contributions arise from MEC in the Siegert's theorem (from 25% at 10 MeV to 260% at 100 MeV). Similar observations have been made by Gari and Hebach[23], by Laget[24] and by others[25]. Additional explicit MEC corrections beyond the Siegert operator becomes significant only near π-threshold. Moreover Fig. 8 shows that E1 contains the dominant MEC effects.

Different potentials seem to give rather similar results though some difference in detail exists[26]. This is shown, concerning the total photodisintegration cross section, in Fig. 9[26] where the results for the Paris potential (Paris) and the Tourreil-Rouben-Sprung potential (dTS) are compared with the result for Reid-soft core potential (RSC).

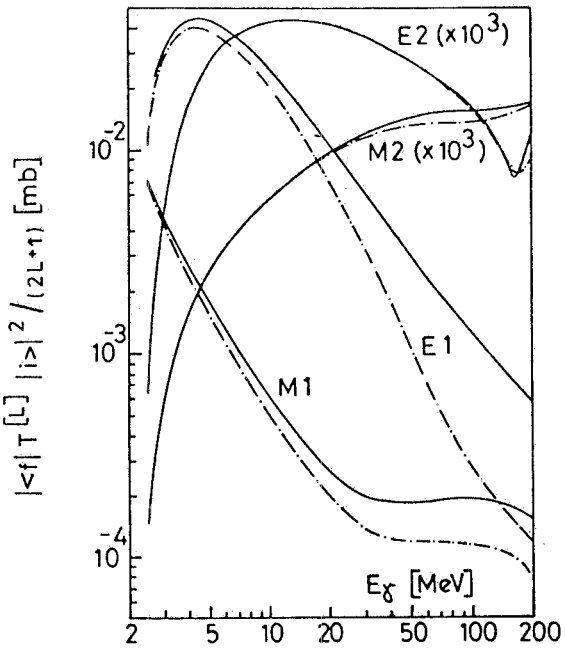

FIG. 8 - Multipole transition strength without (dash-dot curves) and with MEC (full curves) from ref. (19).

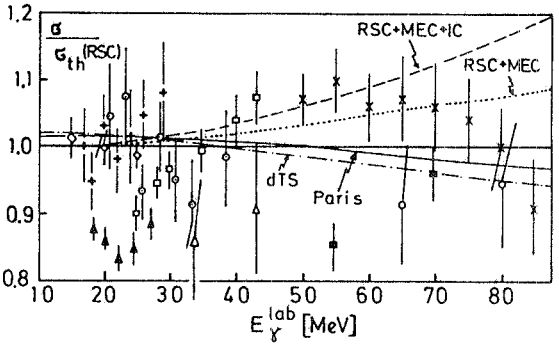

FIG. 9 - Ratio between σ and σ_{th} (RSC) total cross sections from ref. (19). The points show experimental data; the curves represent various potentials and the addition of MEC and IC.

All these calculations are made using only $H^{int}_{[1]}$. Old calculations of the same authors using Hamada-Johnston potential[17] are not reported in the figure. In Fig. 9 are also displayed the influence of the "explicit" exchange effects (RSC+MEC) due to $H^{int}_{[2]}$ and the influence of adding also the isobar configurations (RSC+MEC+IC) and the existing experimental data, that will be discussed in sect. 3, are compared with the theoretical results.

It is evident from Fig. 9 that at intermediate energies the use of different realistic potentials, the addition of "explicit" exchange effect, the introduction of isobar configurations, each of these ingredients contributes to modify the total cross section not more than 10-15% and that only experimental data with an accuracy much better than 10% can provide a test for the different ingredients. This point will be discussed more accurately in section 4.

Very sensitive to the details of the calculations appears to be the differential cross section of $d(\gamma, p)n$ at 0^o. This problem has been studied by several authors[27-32] since experimental results obtained by Hughes et al.[33] in 1976 and more recently confirmed by Gilot et al.[34] differ of about 40% from the theoretical predictions of normal calculations even after the inclusion of the "explicit" exchange current contributions, as shown in Fig. 10. The discrepancy seems to be due to the strength of the tensor part of the NN potential that give the percentual of D-state in the deuteron[27-29, 32], generally overstimated, or to the relativistic contributions to the one- and two-body charge density[30, 31].

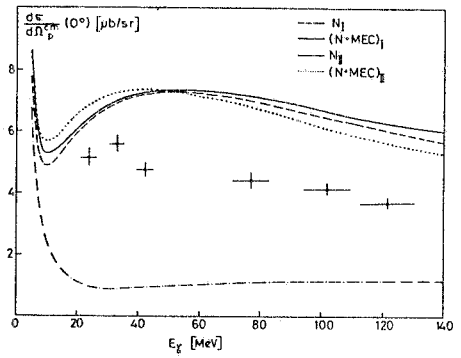

FIG. 10 - Differential cross section of $D(\gamma, p)n$ at 0^o from ref. (19). The experimental points are from refs. (33) and (34). Notation as Fig. 6.

Two methods can be used to introduce the meson exchange current effect and the excitation of the nucleon effect in the photodisintegration of deuteron calculations.

The first one is the classical calculation that introduces explicitely meson current in the interaction Hamiltonian, as already discussed.

The second one is to evaluate the transition amplitude corresponding to each diagram representing deuteron photodisintegration. This method was developed by Laget[24] and in principle, should give the some results as the first one. But there are some differences in the approximations. In Fig. 11 the diagrams that represents deuteron photodisintegration amplitude are presented.

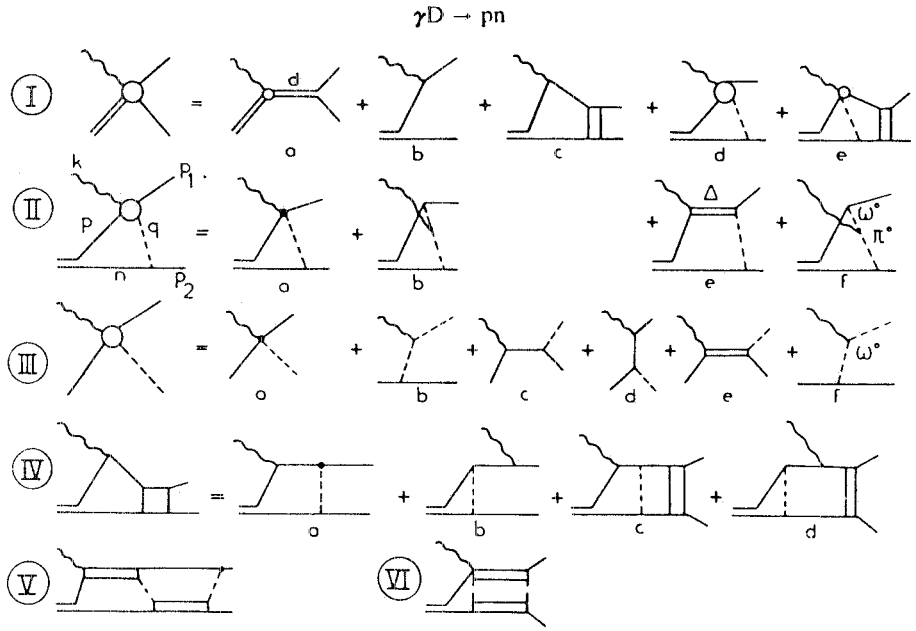

FIG. 11 - The deuteron photodisintegration amplitude is expanded in terms of the leading diagram I. The pion reabsorption amplitude Id is expanded into the relevant diagram II, which come from the expansion III of the elementary $\gamma N \rightarrow \pi N$ amplitude in terms of the Born terms (IIIa,b) the nucleon exchange terms (IIIc,d) the Δ-formation terms (IIIc) and the ω^o exchange term (IIIf). The N-N rescattering amplitude (Ic) is expanded (IV) to show how the nucleon exchange terms are already taken into account (ref. 24).

The first method takes into account multipoles up to $L = 4$ (truncation in the multipole expansion) but corresponds to evaluate the contribution of all the diagrams of Fig.11.

In the second method there is no truncation in the multipole expansion but only the contribution of the one-loop diagram has been evaluated (truncation in the diagram expansion). This means that the interactions in the final state of the system have not been taken into account.

At low energies (20-40 MeV) the results of the two methods are practically identical as shown in Fig. 12. In both cases the calculations are performed using a Reid--soft core potential and a value of $\Lambda_\pi = 5$ fm^{-1} for what concerns the π-baryon form factor (dipole). At higher energies (80-120 MeV) a large discrepancy appears between

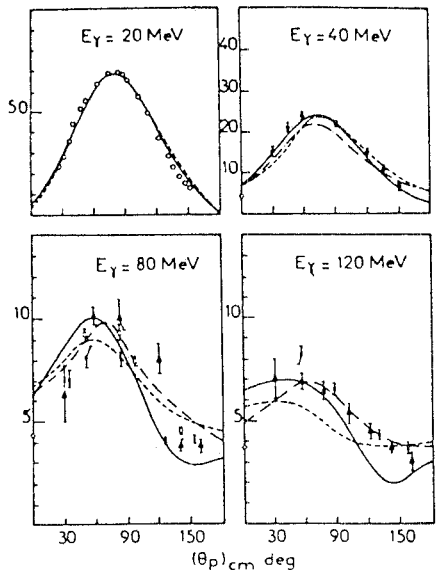

FIG. 12 - Differential cross section for E_γ = 20, 40, 80 and 120 MeV from ref. (24). Comparison between calculations of ref. (24) (full line) and that ones of ref. (19) dot-dashed line) and of ref. (15) (broken line).

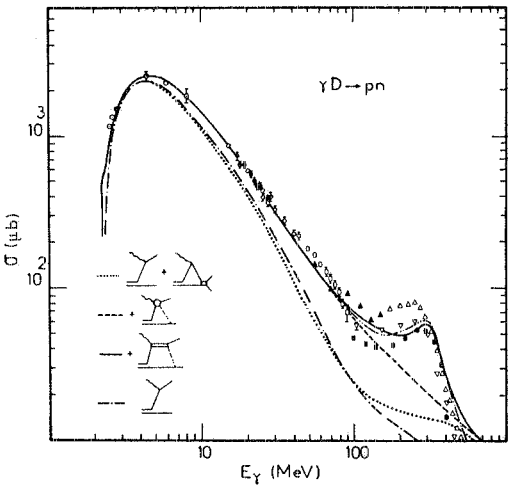

FIG. 13 - Total photodisintegration cross section from ref. (24). The experimental points are from various experiments. The full-line curve is the result of Laget calculations. The other curve show the contribution coming from each diagram of Fig. 11.

the two calculations mainly for what concerns the differential cross section, but this discrepancy recently disappeared since a sign error was found by the author in the amplitude corresponding to the diagram I_b for the interaction with the neutron (expression (6) of ref. (35)).

The agreement between the two calculations in the whole energy range (20-120MeV) proves that in this energy region both the interaction in the final state and the multipole transitions above L = 4 contribute only for few percent.

At high energy all the existing experimental data in the photodisintegration cross section show a resonance at about 300 MeV (Fig. 13) which is clearly associated with baryon resonances observed in other processes (pion-proton scattering, photo-production of pions from nucleons) at corresponding energies.

I will conclude this section with a fast review of the most interesting calculations available on this problem. Around 1955-1956 (just after the first experiments in this energy region) several theoretical approaches have been made to try to reproduce the experimental results. Austern[36] and Feld[37] gave a nuclear isobar interpretation of the 300 MeV resonance. They applied an intermediate state in which one nucleon has been excited to its isobar state $(\frac{3}{2}, \frac{3}{2})$ by M1 photon absorption, and the two nucleons

are in relative S-state. This intermediate state can decay in two different ways: (i) the pion from isobar decay can be absorbed by the other nucleon, leading to photodisintegration of the deuteron, without meson emission; (ii) the pion from the isobar can be scattered by the other nucleon, leading to two nucleons in an S-state, plus a pion.

In Fig. 14 the scheme of the isobar model is presented. The photodisintegration cross section is calculated from detailed balance arguments:

$$\sigma(\gamma + d \rightarrow n + p) = \frac{9}{4}\,\sigma(\gamma + p \rightarrow \pi^{o} + p)\,\frac{\sigma(\pi^{+} + d \rightarrow p + p)}{\sigma(\pi^{+} + p \rightarrow \pi^{+} + p)} \,. \qquad (27)$$

The factor $\frac{9}{4}$ comes from statistical weights; $\sigma(\gamma + p \rightarrow \pi^{o} + p)$ is the cross section for photoproduction of the isobar state; $\sigma(\pi^{+} + d \rightarrow p + p)/\sigma(\pi^{+} + p \rightarrow \pi^{+} + p)$ is proportional to the probability that the isobar will decay by photodisintegration of the deuteron.

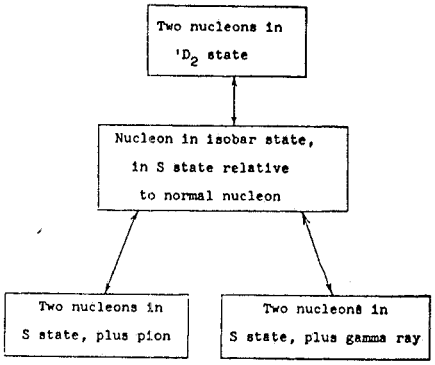

FIG. 14 - The scheme of the isobar model, from ref. (36)

In Fig. 15 is shown the comparison between the results of Austern's calculations and the experimental data. The outstanding discrepancy between experiment and theory occurs between 70 and 300 MeV. At lower energies the disagreement must be expected since the calculations were performed using the Schiff treatment, already presented in this section, that does not take into account any meson exchange effect implicit or explicit. At higher energies were neglected the processes corresponding to production of mesons in S-states i. e. the fact that above 200 MeV the π^{+}-production receives a large contribution from electric dipole γ-ray interaction, involving meson emission in T = $\frac{1}{2}$ states and giving meson S-wave terms. These processes have been taken into account in the calculation of Wilson[38] where the photodisintegration of deuteron is seen as the photoproduction of mesons on a separate nu-

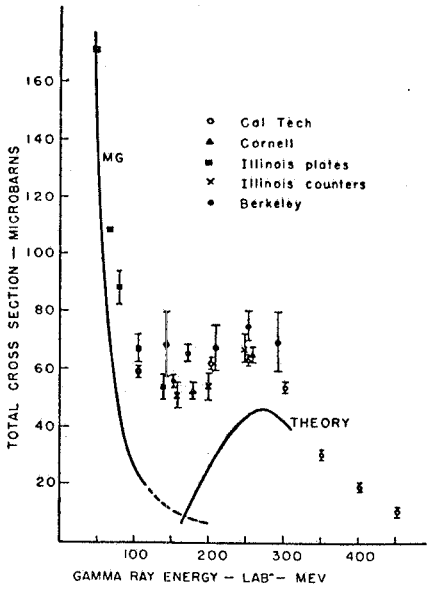

FIG. 15 - Comparison between Austern's calculations for the total cross section and the experimental data, from ref. (36).

cleon and the subsequent reabsorption of the meson by the other nucleon, if the two nucleons are within a distance of about $\hbar/\mu_\pi c$.

In the above picture the total cross section is given by

$$\sigma_d = \sigma(\pi)_{np} P \varrho_{np}/\varrho_\pi \tag{28}$$

where $\sigma(\pi)_{np}$ is the total cross section for production of mesons of any kind on the neutron and proton; P the probability of reabsorption of the meson by the other nucleon roughly given by the fraction of the time that the two nucleons find themselves within a distance of $0.7\hbar/\mu_\pi c$; ϱ_{np} the density of the final states of the two nucleons and the density of the final states of the meson in photoproduction on a single nucleon. Mesons can be produced in S- and P-states. As a consequence the angular distribution is almost isotropic at lower energies and proportional to $(2+3\sin^2\theta)$ at higher energies.

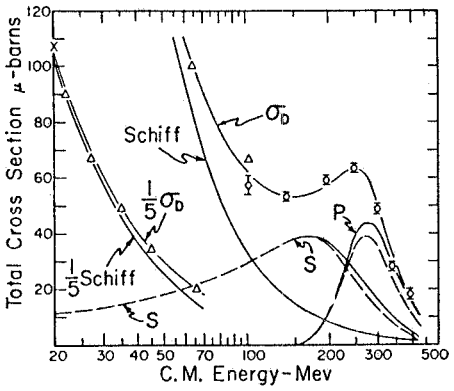

FIG. 16 - Total cross section from ref. (38). Results of Wilson calculations and comparison with Schiff calculations and with experimental data. The contribution of the effect of meson production in S- and P-states is also shown.

A very good agreement between experiment and theory appears in Fig. 16. Unfortunately an error has been made in the comparison, since the experimental energy scale has not been transformed from the laboratory to the C.M. system. This gives a difference in the energy scale which amounts to 36 MeV at 300 MeV.

Zachariasen[39] tried to reproduce the resonance near 300 MeV, by applying the Chew meson theory, and again he was able to reproduce the qualitative features near 300 MeV but not the experimental behaviour at lower energies presumably because again of the neglect of processes corresponding to production of mesons in S-states.

Laget[24] extended the calculations, already discussed in this section, up to 800 MeV. In Fig. 13 the theoretical results for the total cross section are compared with the existing experimental data. Since a vast discrepancy exists between the different experiments it is very hard to say anything about the agreement between experiment and theory.

As a conclusion of this section one can say that the energy region below 80 MeV was sufficiently theoretically investigated and there is a good agreement between the different approaches. At low energy, it means up to 20 MeV, the Schiff's[12] and Marshall and Guth's[13] calculations are a good approximation of the more realistic calculations

of Partovi[15]. Moreover, as the "explicit" meson exchange and the nucleon excitation effects give sensitive contributions only at high energies, Partovi's results are very similar to that ones of more sophisticated calculations[19, 24] at least up to 80 MeV. For what concerns the high energy region, any theory that introduces properly isobar effects seems to be able to reproduce the Δ resonance. On the contrary the intermediate region between 100 and 300 MeV seems to be more sensitive to the different theoretical method and still open to investigations.

3. - PRESENT STATUS OF THE EXPERIMENT

Looking through the literature I found around fifty experiments on the photodisintegration of deuteron between the threshold and 1 GeV and I am sure that many are still missing. But these ones can be in any case a good statistic to have an idea about what is the present status of the experiments in photodisintegration of deuteron. It is convenient for the discussion to divide the experiments in several energy ranges and according to the utilized facility mainly concerning the photon source.

In the energy range near the threshold, i. e. below 3 MeV, almost all the experiments[2, 40-46] used γ-rays from ThC" or ^{24}Na or ^{72}Ga sources. Only one experiment[47] used a continuous photon spectrum obtained by a 3.2 MeV Electrostatic Generator. Some of these experiments[2, 43-46] measured the total cross section, the other ones[40-42, 47] measured the ratio between two differential cross sections $\sigma(0^o)/\sigma(90^o)$ and/or the ratio between the magnetic dipole and electric dipole contribution to the total cross section.

There is a general agreement between the results of the different experiments except for ref. (2), that is the Chadwick and Goldhaber experiment of 1934, already mentioned in section 1. The value of the total cross section measured in this experiment is a factor about 4 lower that of the other experiments. The reason can be that the source was not calibrated and the efficiency of the ionization chamber was not well known.

In the "low energy region", i. e. between 4 and 28 MeV I found fifteen experiments. Five of these[48-52] used monochromatic γ-rays from reaction induced by photons, as follows :

$^{15}N(p, \alpha)^{12}C^*$ $\qquad E_\gamma = 4.45 \pm 0.04$

$^{19}F(p, \alpha)^{16}O^*$ $\qquad E_\gamma = 6.14 \pm 0.01$

$^{9}Be(p, \gamma)^{10}B$ $\qquad E_\gamma = 7.39 \pm 0.15$

$^{13}C(p, \gamma)^{14}N$ $\qquad E_\gamma = 8.14 \pm 0.08$

$^{11}B(p, \gamma)^{12}C$ $\quad E_\gamma = 12.5 \pm 0.21$

$^{7}Li(p, \gamma)^{8}Be$ $\quad E_\gamma = 17.6 \pm 0.20$.

One experiment[53] obtained the deuteron photodisintegration cross section measuring the difference in the photon absorption by normal and heavy water (H_2O and D_2O) absorbers of equal length. A well collimated bremsstrahlung beam intersected two identical magnetic Compton spectrometers, the first of which has been used as a photon flux monitor and the H_2O or D_2O target was between the two spectrometers. In this experiment two possible systematic errors, concerning the absolute cross section value, can arise from the uncertainty in the atomic cross section and from the absolute length of the two absorbers (H_2O and D_2O).

An other experiment[54] extracted the equivalent photon cross section from deuteron electrodisintegration measurements, assuming a virtual photon spectrum in long-wave approximation and relative only to E1 multipolarity. So the main systematic error concerning this experiment results comes from the assumed virtual photon spectrum. All the other experiments in this energy range[55-62] used a normal bremsstrahlung photon beam.

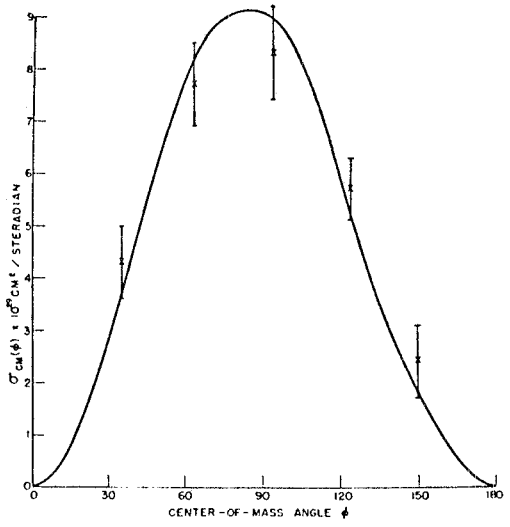

FIG. 17 - Comparison between the experimental differential cross section for photon energy 14.8-17.6 MeV and the Marshall and Guth[13] calculations (full line) from ref. (49).

From what concerns the first group of experiments, one finds a very nice agreement with the Marshall and Guth calculations[13] that, as discussed in section 2, in the low energy region are a good approximation of more sophisticated calculations (refs. (15), (19) and (24)).

As an example Fig. 17 shows the comparison between the absolute differential cross section measured by ref. (49) for photon energy between 14.8 and 17.6 MeV and the calculations of ref. (13). Moreover in the Table I the values of the total cross section, measured by the different experiments at 17.6 MeV photon energy, are presented.

The experiments of refs. (53) and (54) compared their results with the predictions of Partovi[15] and found a very good agreement, as shown in Figs. 18, 19, 20 and 21.

TABLE I

σ_{tot} (17.6 MeV)	Reference
$7.2 \pm 1.5 \times 10^{-28}$ cm^2	(49)
$7.1 \pm 1.5 \times 10^{-28}$ cm^2	(50)
$7.7 \pm 0.9 \times 10^{-28}$ cm^2	(51)
6.7	ref. (13) calculations

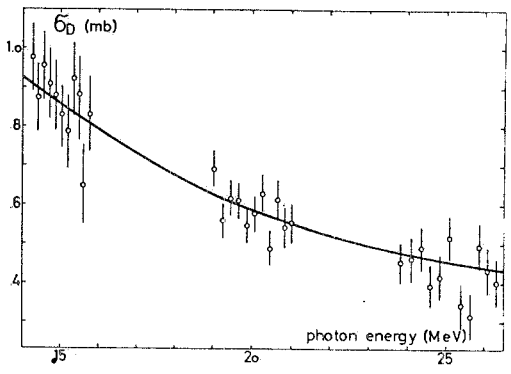

FIG. 18 - The measured total cross section (open circle) of ref. (53) compared with the calculation of Partovi[15] (full line).

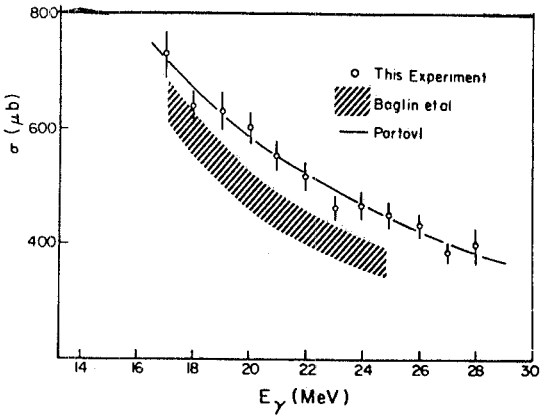

FIG. 19 - Experimental total cross section from ref. (54) (open circle) and from ref. (61) (dashed zone) and comparison with Partovi's calculations (full line).

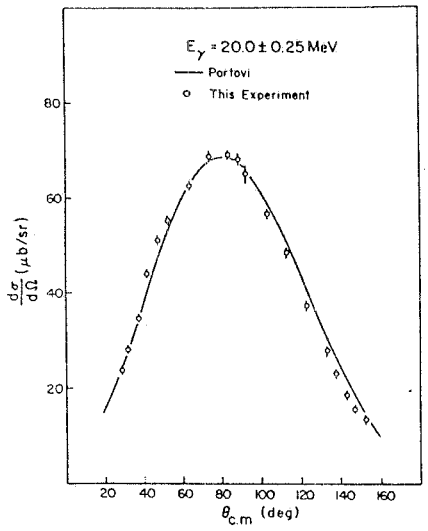

FIG. 20 - Comparison between the differential cross section measured by ref. (54) at E_γ = 20 MeV (open circle) and Partovi's calculations (full line).

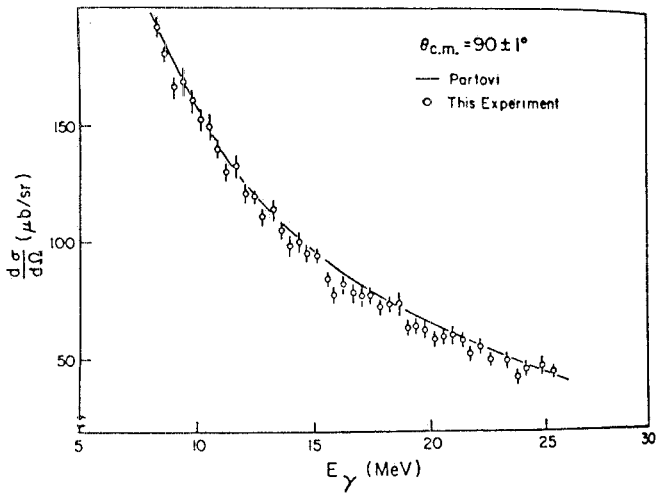

FIG. 21 - Comparison between the differential cross section at a c.m. angle of 90° measured by ref. (54) (open circle) and Partovi's calculations (full line).

If we look at the experiments performed using bremsstrahlung beam we find, as was already shown in Fig. 7, a general disagreement between the different experiments andwith the theoretical calculations mainly for what concerns the absolute value or the behaviour of the total cross section with the energy, but not so large discrepancy between the behaviour of the measured and expected differential cross section, as shown in Fig. 22[59]. The angular distribution was written $W(\theta) = \sum_{n=0}^{3} A_n P_n(\cos\theta)$, where $P_n(\cos\theta)$ are the Legendre polynomials and the ratios A_1/A_0, A_2/A_0 and A_3/A_0 obtained by the fit of the experimental data have been plotted in the figure.

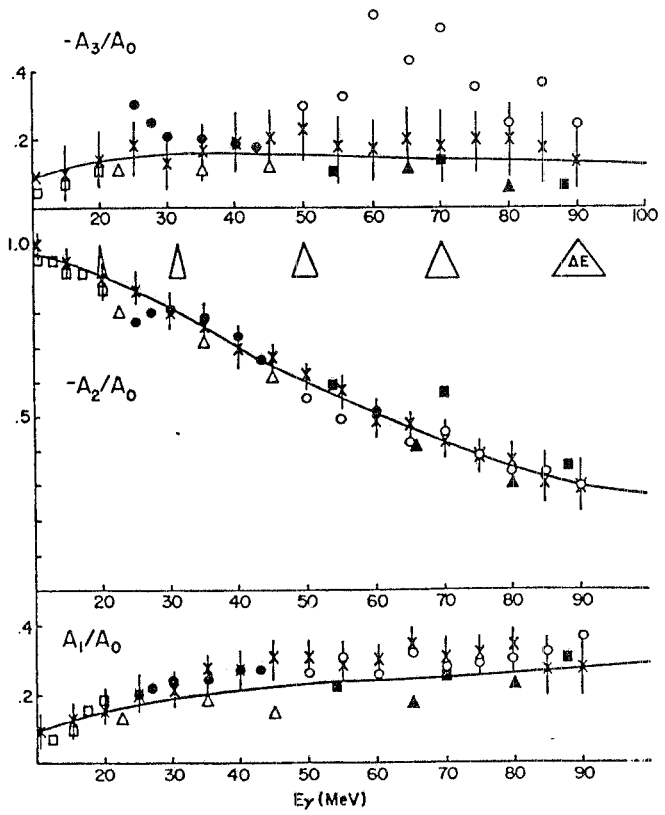

FIG. 22 - Coefficients of Legendre polynomials for the angular distribution of deuteron photodisintegration as described in the text. Comparison between Partovi's calculations (full line) and experimental values of various experiment, from ref. (59).

In the "intermediate energy range", i.e. between 30 and 150 MeV, except the experiment performed at Louvain[63], all the experiments used bremsstrahlung photon beam (refs. 59, 60, 62, 64-68).

In the experiment of ref. (63) the total cross section for radiative neutron-proton capture has been measured, using the monochromatic neutron beam obtained bombarding a lithium target with protons of different energies and selecting the energy of neutrons by time-of-flight measurements. Then the total photodisintegration cross section, into the corresponding energies, has been deduced by application of the detailed balance.

As shown in Fig. 23 the results agree very well with the results of ref. (53) and with the theoretical calculations of Partovi[15], while a large discrepancy exists between the data of these experiments and that ones of ref. (61). For what concerns the other experiments in this energy range I refer myself again to the Fig. 9, that gives alone, without any additional comment, a clear idea of the situation of the experimental data concerning the total photodisintegration cross section of deuteron between 20 and 80 MeV.

On the other side we do not find in Fig. 22, that covers the energy region up to 90 MeV and presents also the results of some experiments in the intermediate energy range, such a large discrepancy between the behaviour of the measured and the expected differential cross section. Moreover in a recent paper[69] the existing data on angular distribution of deuteron photodisintegration between 10 and 120 MeV have been analyzed and compared with a theory including MEC + IC contributions. The differential cross section has been written

$$\frac{d(\theta_{CM})}{d\Omega} = \sum_{i=0}^{A} A_i(E_\gamma)\, P_i(\cos\theta_{CM})$$

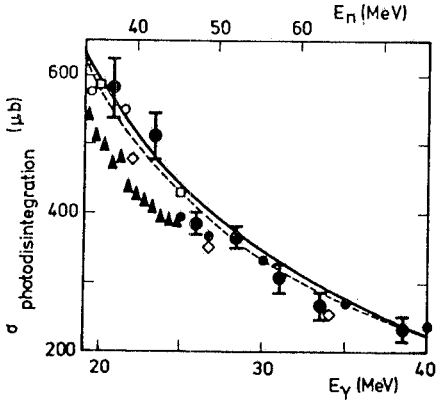

FIG. 23 - Comparison between the experimental total cross section measured by ref. (53) (◇), (61) (▲) and (63) (●) and the prediction of Partovi's calculations (full line), from ref. (63).

(where $P_i(\cos\theta)$ are again the Legendre polynomials) and the authors give the experimental evaluation of the coefficients A_i by fitting all the experimental data. They analyzed about 400 data and the result of the best fit for the A_0, A_1, A_2 and A_3 coefficients are presented in Fig. 24, together with the uncertainty evaluated taking into account both

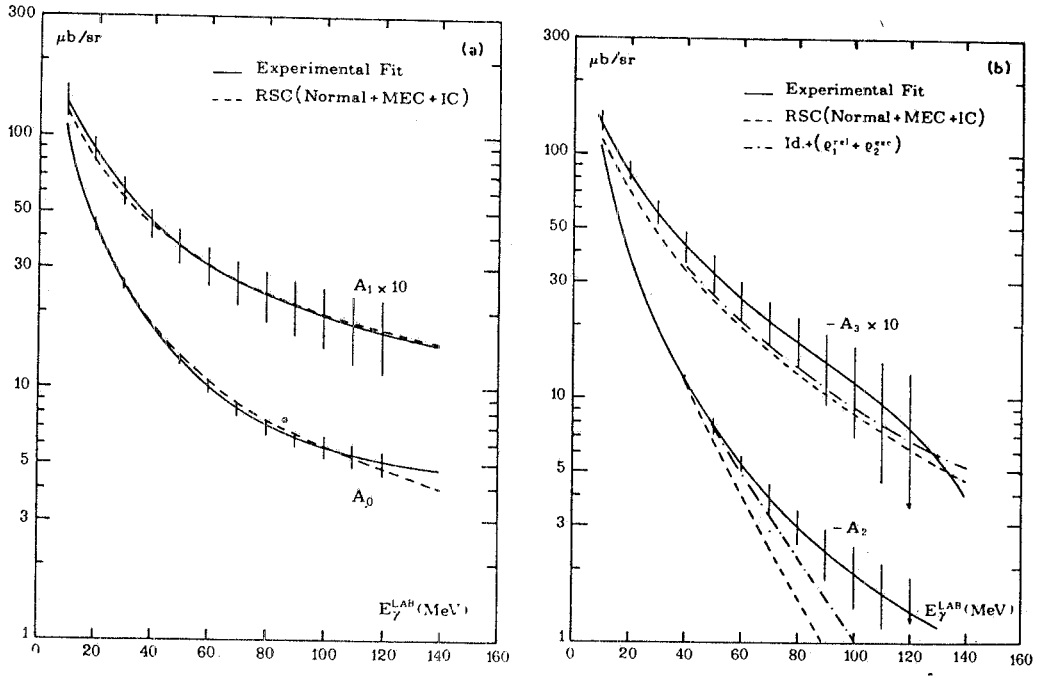

FIG. 24 - Results for the coefficients A_i (i = 0, 3) of the d(γ, p)n angular distribution from ref. (69). The full lines represent the fit of the existing experimental data. The dashed curves are the theoretical results (N+MEC + IC) and the dot-dash-line curves include relativistic correction, as described in ref. (69).

statistical and systematic errors quoted in the different experiments. The relative small uncertainty for the A_i coefficients reported by the authors[69] mainly below 80 MeV, shows once more that the experimental data in this energy region fail mainly for the absolute value of the cross section, while the shape of the differential cross section found in the different experiments is quite the same.

In Fig. 25, again from ref. (69), the ratio between the experimental and theoretical total cross sections is plotted. The experimental cross section was evaluated, as $\sigma_{tot} = 4\pi A_0$, starting from the best-fit value of the A_0 coefficient.

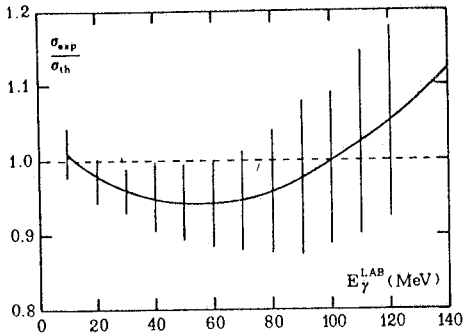

FIG. 25 - Ratio σ_{exp}/σ_{th} between the total cross section obtained by the fit ($\sigma_{exp} = 4\pi A_0$) of the exsisting experimental data and the theoretical prediction including MEC+IC from ref. (69).

In the "high energy region", i. e. between 150 and 450 MeV, except one experiment[70] that used tagged photons, all the experiments[68, 71-81] were performed with normal bremsstrahlung photon beam.

In Figs. 26, 27, 28, 29 and 30 the comparison of the total and differential cross sections measured by various experiments is reported. A large discrepancy appears between the different measurements (Figs. 26, 27 and 28), even if some of them agree each other, as shown in Figs. 29 and 30. Again if we compare the behaviour of the various measured differential cross sections, the discrepancy in the behaviour is not so large at least up to 400 MeV, as shown in Figs. 31 and 32[70]. For what concerns Fig. 31, the angular distribution was written

$$\frac{d\sigma(\theta_{CM})}{d\Omega} = A + B\cos\theta_{CM} + C\cos^2\theta_{CM}$$

and the ratios between the coefficients B/A and C/A have been plotted. Fig. 32 shows the relative angular distribution for various experiments, it means that the data have been normalized to the same 4π value.

In the "very high energy region", i. e. between 500 and 1000 MeV there are only two experiments[82, 83]. They have been performed using bremsstrahlung photon beam and both measured the differential cross section at around 90° in the c. m. system and did not find evidence of any resonant behaviour of the cross section in this energy re-

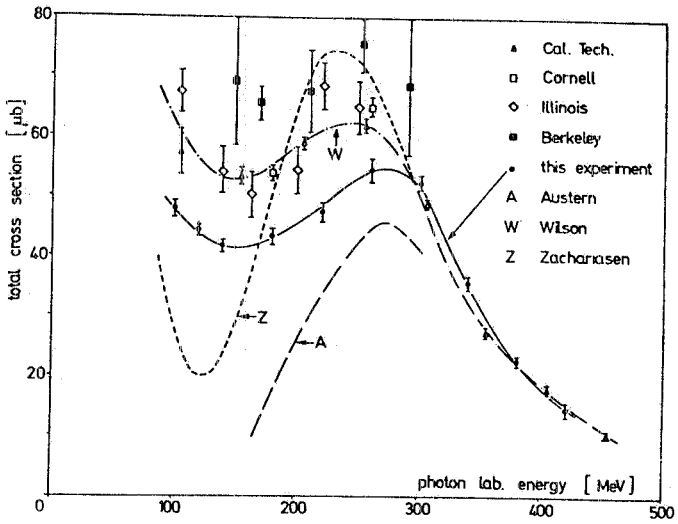

FIG. 26 - Comparison between the total cross section measured in various experiments and the theoretical predictions of refs. (36), (38) and (39) from ref. (76).

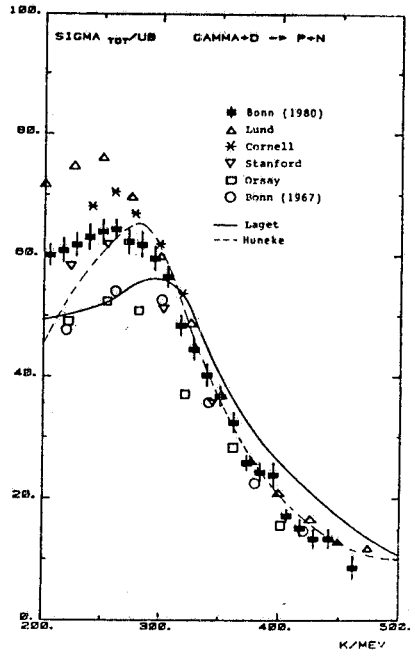

FIG. 27 - Comparison between the total cross section measured in various experiments and the theoretical predictions of refs. (35) and (70).

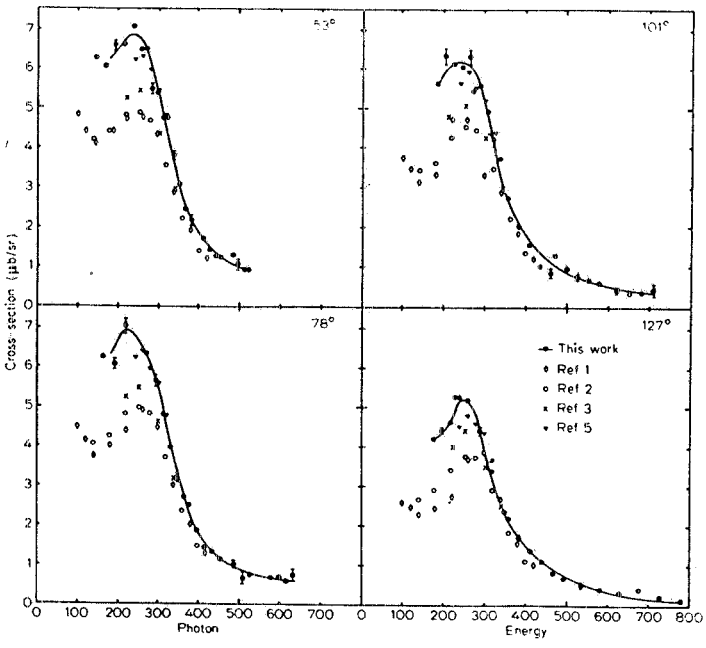

FIG. 28 - Differential cross section at proton c. m. angles of 53°, 78°, 101° and 127° from ref. (80b). Comparison between the data of ref. (80) and other values reported in the literature.

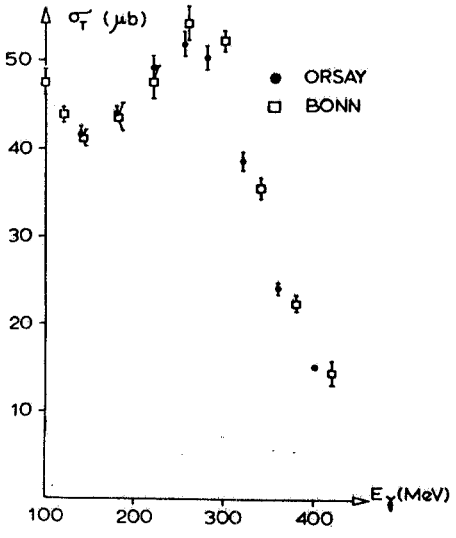

FIG. 29 - Total cross section between 100 and 400 MeV. Comparison between the experimental values of ref. (76) and that ones of ref. (77).

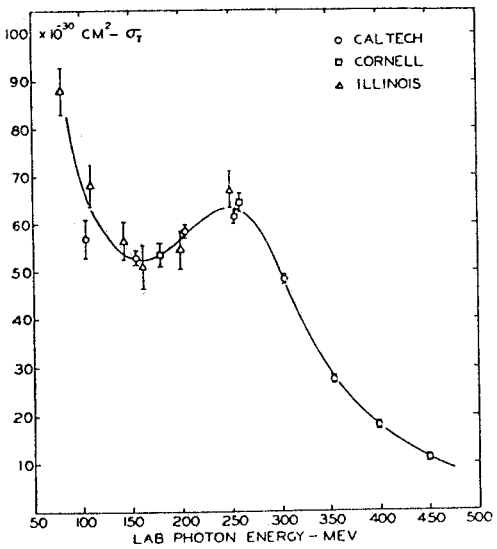

FIG. 30 - Total cross section between 100 and 400 MeV. Comparison between the experimental values of refs. (65), (73) and (78).

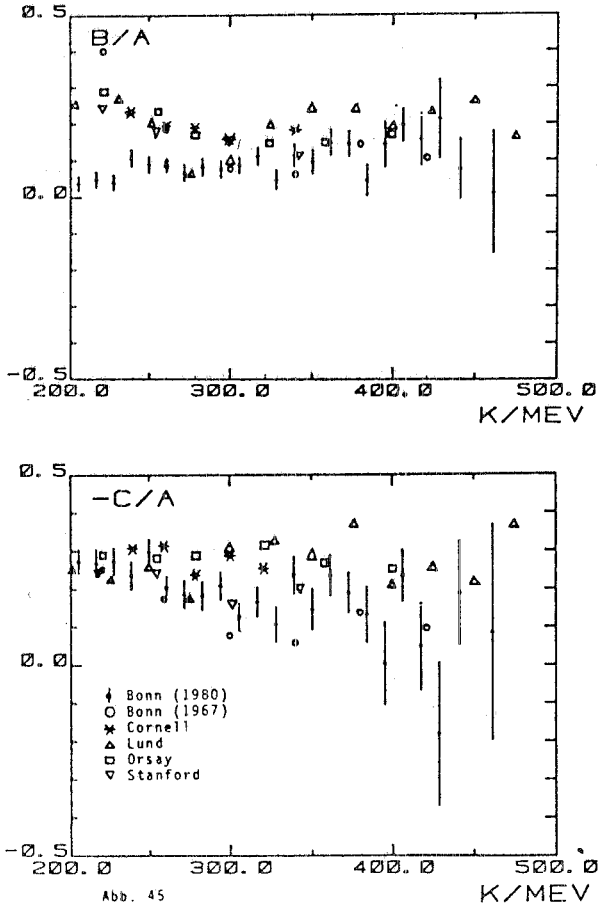

FIG. 31 - Ratio between the coefficients of the angular distribution $d\sigma(\theta)/d\Omega = A + B\cos\theta + C\cos^2\theta$ (in the c.m. system) measured in various experiments from ref. (70).

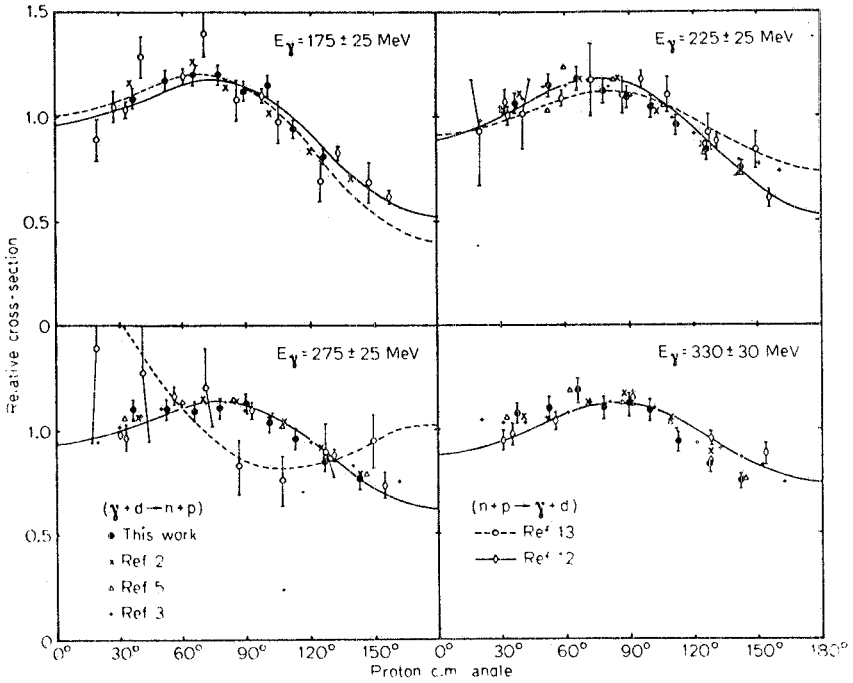

FIG. 32 - Relative angular distributions for the reactions $\gamma + d \rightarrow n + p$ measured in various experiments at E_γ = 175, 225, 275 and 330 MeV, from ref. (80).

gion. The more extensive results of ref. (83) do not differ so much (they are about 20% higher) from the results of ref. (82) that are in good agreement with the results of ref. (73) at lower energies.

I will conclude this section with some general remarks and comments concerning the results of the reported experiments.

In the whole energy range, starting from the threshold of deuteron photodisintegration up to high energies, one finds discrepancy in the absolute value of the cross section measured by various experiments but generally not so much disagreement for what concerns the relative behaviour of the total cross section with the energy, the position of the Δ-resonance, the relative behaviour of the angular distribution.

One deduces therefore that the main reasons for the disagreement of the absolute value can be the lack of a good knowledge of the incoming photon flux and of the effective thickness of the deuteron target or of the absolute value of the detector efficiency.

As I already said at the beginning of section 1 deuteron target is a difficult target. The most part of the experiments used a gas target or deuterated water or paraffin and only few experiments used a liquid deuteron target. But it is well known that gas or enriched targets are not so easy to be produced. Moreover it is difficult and sometime impossible to report and to make comments on the detection apparatus used if one does not know the reliability tests performed in each experiment.

But on the contrary it is possible to make some general remarks concerning the knowledge of the photon flux. The largest disagreement in the absolute values appears between experiments performed with bremsstrahlung beam, i. e. when only a little fraction of the incoming beam power is utilized. In these cases a little uncertainty in the knowledge of the bremsstrahlung spectrum can produce a big error in the intensity of the utilized photons.

As shown in Fig. 33 from ref. (84), different calculations of the bremsstrahlung process produce only a little difference on the cross section integrated over the photon angle, while a large discrepancy exists in the differential cross section with respect to the photon angle predicted by various calculations. This means that when in the experiment the photon beam has no collimation or a very large collimation, any bremsstrahlung spectrum calculation gives suitable results. On the contrary when, due to a severe collimation, it is necessary to known the real angular distribution, different calculations can give different results and the difference depends on the experimental conditions.

In almost all the experiments the Schiff[85] bremsstrahlung formula, that has a relative simple analytic form, has been extensively used to evaluate the flux of the to

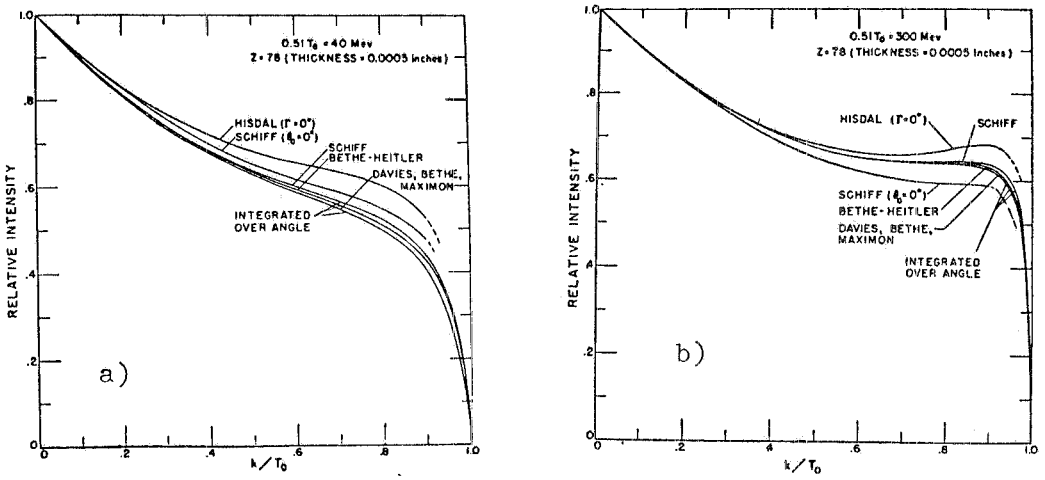

FIG. 33 - Comparison of 40 MeV (a) and 300 MeV (b) bremsstrahlung spectrum shapes predicted by various calculations from ref. (84).

total incoming beam and to estimate the intensity of the utilized photons. Fig. 34 shows the comparison between the measured photon energy spectrum obtained by positrons of 200 MeV on a liquid hydrogen target and the prediction of Schiff's calculation for the bremsstrahlung spectrum[86]. A very good agreement appears within the experimental errors between measured and evaluated photon spectra.

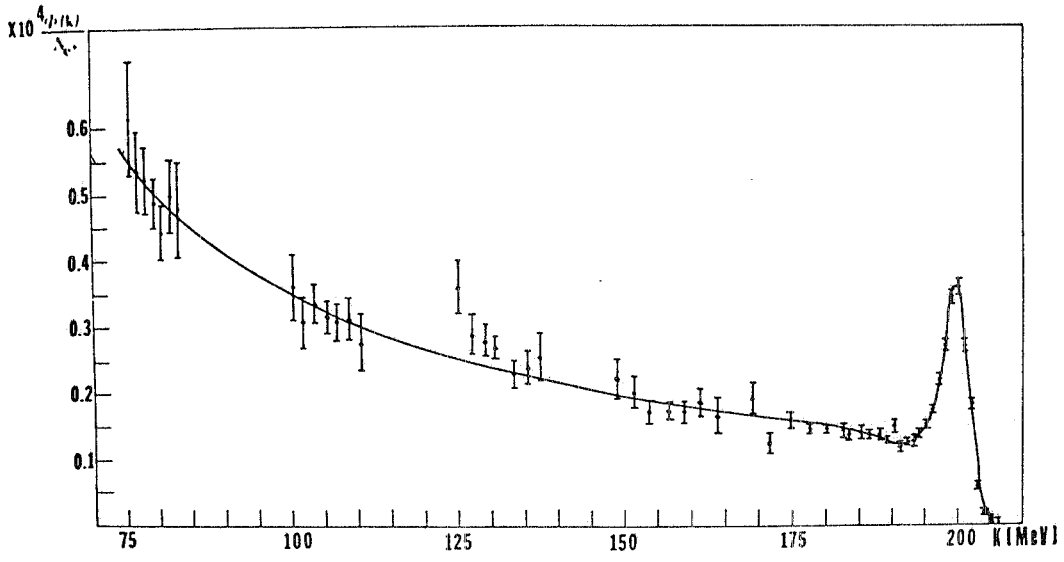

FIG. 34 - Comparison between the measured photon energy spectrum obtained by positron of 200 MeV on a liquid hydrogen target and the prediction (full line) of a calculation using Schiff's formula[86] for the bremsstrahlung cross section.

In the Schiff's calculation a complete screening effect has been considered. A more accurate treatment assuming an intermediate screening effect has been perform

ed by Olsen and Maximon[87]. They included the Coulomb corrections and introduced the Thomas-Fermi atomic form factor to reproduce the electron charge distribution.

In Figs. 35 and 36 is plotted the ratio between the photon energy spectra obtained by electron of 30 and 50 MeV respectively on a beryllium and a copper target, measured by ref. (88).

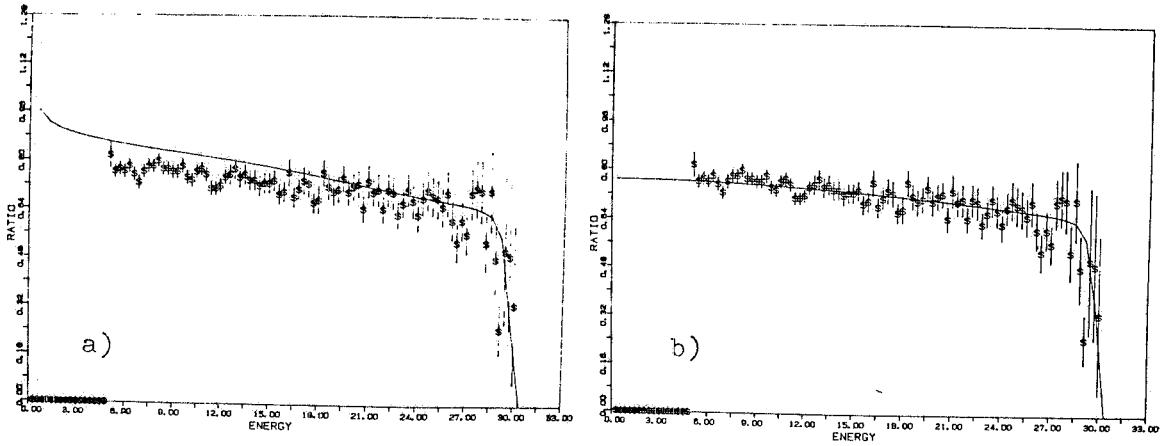

FIG. 35 - Ratio between the photon energy spectra obtained by electron of 30 MeV respectively on Berillium and a Copper target measured by ref. (88). The full line is the prediction of a calculation using Schiff's formula[85] (a), and Olsen and Maximon formula[87] (b) for the bremsstrahlung cross section.

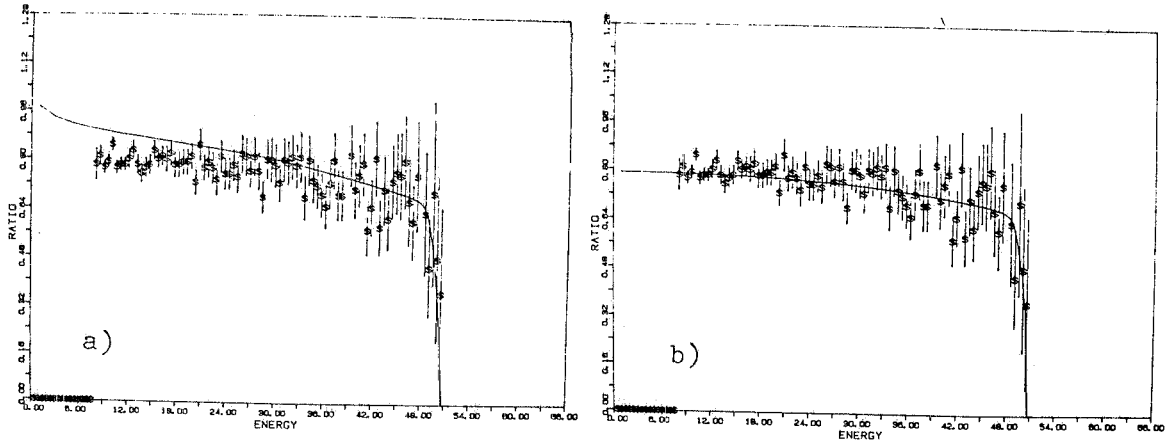

FIG. 36 - The same of Fig. 35 for electron of 50 MeV.

The experimental ratio is compared with the prediction of Schiff's and Olsen and Maximon calculations. This quantity, that in absence of screening effect and Coulomb corrections should be independent of the photon energy, is very sensitive to the corrections and it is therefore a very good test of the validity of the assumed approximations. As the screening effect and the Coulomb corrections produce a distortion in the photon spectrum that depends on the Z of the bremsstrahlung target, the difference in the

absolute value of the utilized photon flux evaluated in the experiments can be due to the different approximations used and/or to the use of different Z targets.

4. - CONCLUSIONS

In spite of the great production of experimental works, due to the large discrepancy between the data, the present status of deuteron photodisintegration experiments does not allow to test the validity of the various theoretical approaches that give in the energy range between 80 and 300 MeV a sensitive difference in the predicted cross section. Therefore one can conclude that the photodisintegration of deuteron at intermediate energies is still open to experimental investigation. To test the validity of different calculations very precise measurements of the absolute value of the differential and total cross section are necessary.

Moreover, as any realistic theory gives confrontable results below 80 MeV, it should be very important to perform an experiment spanning the energy region between at least 50 and 300 MeV with the same technique, to have a test of the reliability of the absolute value of the experimental results.

REFERENCES

(1) - E. Hadjimichael and D. P. Saylor, Phys. Rev. Letters 45, 1776 (1980).

(2) - J. Chadwick and M. Goldhaber, Nature 134, 237 (1934).

(3) - J. Chadwick, Nature 129, 469 (1932).

(4) - W. Heisenberg, Zeits. für Physik 77, 1 (1932); 78, 156 (1932); 80, 587 (1932).

(5) - E. Majorana, Zeits. für Physik 82, 137 (1933).

(6) - E. Wigner, Zeits. für Physik 83, 253 (1933); Phys. Rev. 43, 252 (1933).

(7) - H. A. Bethe and R. E. Peierls, Proc. Roy. Soc. A148, 146 (1935).

(8) - H. A. Bethe and C. Longmire, Phys. Rev. 77, 647 (1950).

(9) - F. C. Barber and R. E. Peierls, Phys. Rev. 75, 312 (1949).

(10) - J. M. Blatt and J. D. Jackson, Phys. Rev. 76, 18 (1949).

(11) - J. S. Levinger, Phys. Rev. 76, 699 (1949).

(12) - L. I. Schiff, Phys. Rev. 78, 733 (1950).

(13) - J. F. Marshall and E. Guth, Phys. Rev. 78, 738 (1950).

(14) - J. S. Levinger, Nuclear Photodisintegration (Oxford University Press, 1960), Chap. II.

(15) - F. Partovi, Annals of Physics 27, 79 (1964).

(16) - T. Hamada and I. D. Johnston, Nuclear Phys. 34, 382 (1962).

(17) - H. G. Miller and H. Arenhövel, Phys. Rev. C7, 1003 (1973); H. Arenhövel, W. Fabian and H. G. Miller, Phys. Letters 52B, 303 (1974).

(18) - W. Fabian and H. Arenhövel, Nuclear Phys. A258, 461 (1976); A292, 429 (1977); Lecture Notes in Physics (Springer Verlag, 1978), Vol. 86, pag. 84; H. J. Weber and H. Arenhövel, Phys. Reports 36C, 277 (1978).

(19) - H. Arenhövel, Lecture Notes in Physics (Springer Verlag, 1980), Vol. 137, pag. 136; Proceedings Intern. School of Intermediate Energy Nuclear Physics (Verona, 1981); World Scientific (Singapore, 1982), pag. 103; Nuclear Phys. A374, 521 (1982).

(20) - D. O. Riska and G. E. Brown, Phys. Letters 38B, 193 (1972).

(21) - A. J. F. Siegert, Phys. Rev. 52, 787 (1937); R. G. Sachs, Nuclear Theory (Addison Wesley Publishing, 1953), Chap. 9.

(22) - H. Arenhövel, Zeits. für Physik, A302, 25 (1981).

(23) - M. Gari and H. Hebach, preprint Bochum (1980).

(24) - J. M. Laget, Nuclear Phys. A312, 265 (1978).

(25) - W. Y. P. Hwang and G. A. Miller, Phys. Rev. C22, 968 (1980).

(26) - H. Arenhövel, Phys. Rev. Letters 47, 749 (1981).

(27) - H. Arenhövel and W. Fabian, Nuclear Phys. A282, 397 (1977).

(28) - E. L. Lomon, Phys. Letters B68, 419 (1977).

(29) - M. E. Schulze, D. P. Saylor and R. Goloskie, preprint Worcester Polytechnic Institute (1981).

(30) - W. Jaus and W. S. Woolcook, Nuclear Phys. A365, 477 (1981).

(31) - A. Cambi, B. Mosconi and P. Ricci, Phys. Rev. Letters 48, 462 (1982).

(32) - H. Arenhövel, Proceedings Workshop on Medium Energy Interaction in Nuclear Physics, Pavia, 1982, in press.

(33) - R. Hughes, A. Zieger, H. Wäffler and B. Ziegler, Nuclear Phys. A267, 329 (1976).

(34) - J. F. Gilot, A. Bol, P. Leleux, P. Lipnik and P. Macq, Phys. Rev. Letters 47, 304 (1981).

(35) - J. M. Laget, private communication.

(36) - N. Austern, Phys. Rev. 100, 1522 (1955).

(37) - B. T. Feld, Nuovo Cimento 2, 145 (1955).

(38) - R. R. Wilson, Phys. Rev. 104, 218 (1956).

(39) - F. Zachariasen, Phys. Rev. 101, 371 (1956).

(40) - N. O. Lassen, Phys. Rev. 75, 1099 (1949).

(41) - E. P. Meiners Jr., Phys. Rev. 76, 259 (1949).

(42) - B. Hammermesh and A. Wattenberg, Phys. Rev. 76, 1408 (1949).

(43) - G. R. Bishop, G. R. Collie, C. H. Halban, H. Hedgran, A. Siegbahn, K. du Toit and S. Wilson, Phys. Rev. 80, 211 (1950).

(44) - A. H. Snell, E. C. Barber and R. L. Sternberg, Phys. Rev. 80, 637 (1950).

(45) - S. A. Colgate, Phys. Rev. 83, 1262 (1951).

(46) - P. Marin, G. R. Bishop and H. Halban, Proc. Roy. Soc. A66, 608 (1953); A67, 1113 (1954).

(47) - W. M. Woodward and I. Halpern, Phys. Rev. 76, 107 (1949).

(48) - A. Phillips and J. S. Lawson, Phys. Rev. 80, 326 (1950).

(49) - P. V. C. Hough, Phys. Rev. 80, 1069 (1950).

(50) - H. Wäffler and S. Younis, Helv. Phys. Acta 24, 483 (1951).

(51) - J. H. Carver and D. H. Wilkinson, Nature 167, 154 (1951).

(52) - a) C. A. Barnes, G. H. Stafford and D. M. Wilkinson, Nature 165, 69 (1950);
b) J. M. Carven and D. M. Wilkinson, Nature 167, 154 (1951);
c) D. M. Wilkinson, Phys. Rev. 86, 373 (1952).

(53) - J. Ahrens, H. B. Eppler, H. Gimm, M. Kröning, P. Riehn, H. Wäffler, A. Zieger and B. Ziegler, Phys. Letters 52B, 49 (1947).

(54) - D. M. Skopik, Y. M. Shin, M. C. Phenneger and J. J. Murphy, Phys. Rev. C9, 531 (1974).

(55) - E. G. Fuller, Phys. Rev. 79, 303 (1950).

(56) - N. E. Krohn Jr. and E. F. Shrader, Phys. Rev. 86, 391 (1952).

(57) - J. Halpern and E. V. Weinstock, Phys. Rev. 91, 934 (1953).

(58) - A. Whetstone and J. Halpern, Phys. Rev. 109, 2072 (1958).

(59) - Y. M. Shin, J. A. Rawlins, W. Buss and A. O. Evwaraye, Nuclear Phys. A154, 482 (1970).

(60) - K. Tietze, H. Reich and J. O. Trier, Zeits. für Physik 242, 328 (1971).

(61) - J. E. E. Baglin, R. W. Carr, E. J. Bentz Jr. and C. P. Wu, Nuclear Phys. A201, 593 (1973).

(62) - B. Weissman and H. L. Schultz, Nuclear Phys. A174, 129 (1971).

(63) - M. Bosman, A. Bol, J. F. Gilot, P. Leleux, P. Lipnix and P. Macq, Phys. Letters 82, 212 (1979).

(64) - L. Allen Jr., Phys. Rev. 98, 705 (1955).

(65) - E. A. Whalin, B. D. Schriever and A. O. Hanson, Phys. Rev. 101, 377 (1956).

(66) - Y. A. Aleksandrov, N. B. Delone, L. I. Slovokhotov, G. A. Sokol and L. N. Shtarkov, Soviet Phys. -JETP 6, 472 (1958).

(67) - J. A. Galey, Phys. Rev. 117, 763 (1960).

(68) - A. M. Smith, S. J. Hall, B. Mann and D. T. Steward, J. Phys. (Proc. Phys. Soc.) Ser. 2A, 1, 553 (1968).

(69) - M. P. De Pascale, G. Giordano, G. Matone, P. Picozza, L. Azario, R. Caloi, L. Casano, L. Ingrosso, M. Mattioli, E. Poldi, D. Prosperi and C. Schaerf, Phys. Letters 119B, 30 (1982).

(70) - a) A. Voswinkel, Diplomarbeit, Bonn 1980;
b) B. Mecking, private communication.

(71) - K. Baba, I. Endo, H. Fukuma, K. Inoue, T. Kawamoto, T. Ohsugi, Y. Sumi, T. Takeshita, S. Uehara and Y. Yamo, Phys. Rev. Letters 48, 729 (1982).

(72) - J. C. Keck, R. M. Littauer, G. K. O'Neill, A. M. Perry and W. M. Woodward, Phys. Rev. 93, 827 (1954).

(73) - J. C. Keck and A. V. Tollestrup, Phys. Rev. 101, 360 (1956).

(74) - D. R. Dixon and K. C. Bandtel, Phys. Rev. 104, 1730 (1956).

(75) - C. A. Tatro, T. R. Palfrey Jr., R. M. Whaley and R. O. Haxby, Phys. Rev. 112, 932 (1958).

(76) - R. Kose, W. Paul, K. Stockhorst and K. H. Kissler, Zeits. für Physik 202, 364 (1967).

(77) - J. Buon, V. Gracco, J. Lefrancois, P. Lehmann, B. Merkel and P. Roy, Phys. Letters 26B, 595 (1968).

(78) - D. I. Sober, D. G. Cassel, A. J. Sadoff, K. W. Chen and P. A. Crean, Phys. Rev. Letters 22, 430 (1969).

(79) - R. L. Anderson, R. Prepost and B. H. Wiik, Phys. Rev. Letters 22, 651 (1969).

(80) - a) P. Dougan, V. Ramsay and W. Stiefler, Report LUSY 7506 (1975);
b) P. Dougan, T. Kivikas, K. Lugner, V. Ramsay and W. Stiefler, Zeits. für Physik A276, 55 (1976).

(81) - B. C. Craft, Proceedings of the Microconference on Study of Few Body Systems with Electromagnetic Probes, Amsterdam (1981), pag. 169; private communication.

(82) - H. Myers, R. Gomez, D. Guinier and A. V. Tollestrup, Phys. Rev. 121, 630 (1961).

(83) - R. Ching and C. Schaerf, Phys. Rev. 141, 1320 (1966).

(84) - H. W. Koch and J. W. Motz, Rev. Mod. Phys. 31, 920 (1959).

(85) - L. I. Schiff, Phys. Rev. 83, 252 (1951).

(86) - G. P. Capitani, E. De Sanctis, P. Di Giacomo, C. Guaraldo, S. Gentile, V. Lucherini, E. Polli, A. R. Reolon and R. Scrimaglio, Nuclear Instr. and Meth. 178, 61 (1980); G. P. Capitani, E. De Sanctis, P. Di Giacomo, C. Guaraldo, V. Lucherini, E. Polli, A. R. Reolon and V. Bellini, Nuclear Instr. and Meth. 203, 353 (1982).

(87) - H. Olsen and L. C. Maximon, Phys. Rev. 114, 887 (1959).

(88) - R. Leicht, K. P. Schelhaas, M. Hammen, J. Ahrens and B. Ziegler, Nuclear Instr. and Meth. 179, 131 (1981).